INFN - Laboratori Nazionali di Frascati
Servizio Documentazione

LNF-91/026 (P)
21 Maggio 1991

$Z^0\gamma^*$ Production at Hadron Colliders

A. Grau
Universitat Autònoma de Barcelona, 08193 Bellaterra, Spain

G. Pancheri
INFN, Laboratori Nazionali di Frascati, P.O.Box 13, 00044 Frascati, Italy

and

Y.N.Srivastava
INFN, University of Perugia, Perugia, Italy

Abstract

We calculate the production of a $Z^0\gamma^*$ pair at hadron colliders from gluon-gluon fusion and quark-antiquark annihilation. We show that the gluon- gluon contribution is always much smaller than the one from quark-antiquark annihilation and compare both to the cross-section for production of an intermediate Higgs boson decaying into a pair of Z^0's , one of them being produced off-the-mass-shell.

1 Introduction

In this paper we calculate the contribution of gluon gluon-scattering to the production of a $Z^0\gamma^*$ pair at hadron colliders and compare it with the contribution coming from quark-antiquark annihilation. These processes are potentially interesting as they constitute part of the background to the production of an intermediate mass Higgs boson, i.e. one such that $m_Z \leq m_H \leq 2m_W$. A Higgs boson in this mass range has a finite probability to decay into a pair of Z^0's, one of which is produced off-the mass-shell. Detection of the Higgs boson in this mass range through its decay into two lepton pairs from the Z^0Z^* final state, has been proposed [1, 2, 3].

There exist diverse theoretical models and arguments which favour this particular mass range. We mention just a few. Non-perturbative results in pure ϕ^4 models [4] imply an upper limit $m_H < 630\ GeV$ under rather general assumptions, but also the much more stringent limit, $m_H < 145\ GeV$ if the regularization cut-off is chosen to be at its natural value $\Lambda = 1.2\ 10^{19}\ GeV$. Recent estimates of higher order radiative corrections to the Electroweak parameters from the high precision LEP results have restricted the range of the top mass and that of the Higgs mass as well [5]. In ref.5, the favourite value for the top mass is $m_t = 122 \pm 35\ GeV$, to which there correspond a minimum of the χ^2 for the Higgs mass which falls in the range below and just above 100 GeV. An exploration of this mass range is also important for the Higgs sector of the Minimal Supersymmetric Standard Model (MSSM). This model predicts a neutral Higgs of mass less than m_Z [3, 6], although radiative corrections [7, 8] tend to shift this mass prediction towards higher mass values. In any event, an estimate of the background processes to the production of the Standard Model Higgs in the 100-200 GeV mass range, becomes important for studying the Higgs sector of Supersymmetric Theories, especially in view of possible additional evidence for a Supersymmetry scale in this mass region, as suggested by the analysis of LEP data by Amaldi et al. [9].

Background to the detection of a neutral Higgs boson decaying in two lepton pairs through the Z^0Z^* channel, comes from many different sources. We recall in particular the one from $Zb\bar{b}$ production which gives a Z^0 accompanied by a μpair. A through analysis of this type of background can be found in ref.10. Here we discuss contributions to the intrinsic background constituted by processes which have the same exclusive final state as the signal under examination.

For the process

$$pp \to H + X \to Z^0Z^* + X \to l_1^+ l_2^- l_3^+ l_4^- + X$$

contributions to the intrinsic background come from

$$q\bar{q} \to Z^0Z^* \tag{1.1}$$

$$q\bar{q} \to Z^0\gamma^* \tag{1.2}$$

$$gluon\ gluon \to Z^0Z^* \tag{1.3}$$

$$gluon\ gluon \to Z^0\gamma^* \tag{1.4}$$

Since the decay channels of interest for experimental purposes, i.e. decay into two lepton pairs, do not distinguish between a virtual photon or a virtual Z^0, all of these processes constitute a potential background. The analytical expressions for the amplitudes for processes (1.1) and (1.2) are in the literature [11, 12]. We present here the amplitude for process (1.4).

In section 2 we present the cross-section for the gluon-gluon contribution to $Z^0\gamma^*$. Our calculation relies on the results of ref.13. In section 3 we do a numerical estimate of this contribution and compare it with the cross-section for process (1.2). Since gluon densities in the x-range of interest are rather large at the LHC and SSC, the possibility that this contribution compares with that from $q\bar{q}$ could not a priori be excluded. Indeed, above the 2 Z^0's threshold, Glover and Van der Bij [14] have shown that the gluonic contribution to Z^0 pair production is between 30 (at the LHC) and 70 percent (at SSC) of that from quarks. For $Z^0\gamma^*$ production, on the other hand, we find that the gluonic contribution is much smaller than the one from quark-antiquark annihilation. The physics reason for this difference is charge conjugation symmetry for the process (1.4). The gluonic process proceeds via an intermediate quark loop [see Fig.1], for which only the vector part of the Z^0 coupling to the quarks survives due to C-invariance.

In section 4 we examine the background processes together with the signal and discuss the necessary cuts, which improve the signal and eliminate the intrinsic unwanted background.

2 Cross Section for $gg \to Z^0\gamma^* \to Z^0\mu^+\mu^-$

There are six diagrams contributing to this process. In fig.(1a) we show three of them, the other three are obtained by permutation of the gluon lines. Notice that from C-invariance only the vector part of the Z^0 coupling to the quarks, g_v^q, contributes to the box diagrams. The matrix element can be written as

$$\mathcal{M}^{\alpha\beta}_{\lambda_2\lambda_3\lambda_4} = \sum_q \frac{eg_s^2 gQ_q}{cos\theta_w}(g_v^q)\frac{\delta^{\alpha\beta}}{2}\frac{e}{k_1^2}\bar{u}(p_1)\gamma^\mu v(p_2)A_\mu^{(\lambda_2\lambda_3\lambda_4)}$$

where α, β are the color indices of the two initial gluons and

$$A_\mu^{(\lambda_2\lambda_3\lambda_4)} = \int \frac{d^4p}{(2\pi)^4}Tr\left\{\gamma_\mu\frac{i}{(\not{p}-m_q)}\gamma_\nu\frac{i}{(\not{p}-\not{k}_2-m_q)}\gamma_\sigma\frac{i}{(\not{p}+\not{k}_1+\not{k}_3-m_q)}\right.$$

$$\left.\gamma_\rho\frac{i}{(\not{p}+\not{k}_1-m_q)}\right\} b_2^{*\nu}(\lambda_2)\; a_3^\rho(\lambda_3)\; a_4^\sigma(\lambda_4) + crossed\ diagrams \qquad (2.1)$$

with $b_2(\lambda_2)$, $a_3(\lambda_3)$, $a_4(\lambda_4)$ the polarization vectors of the Z^0 and the gluons respectively.

The basic cross-section for $gg \to Z^0\gamma^* \to Z^0\mu^+\mu^-$ is given by

$$d\hat{\sigma} = \frac{1}{2\lambda^{1/2}(\hat{s},m_a^2,m_b^2)}\frac{(2\pi)^4\sum|\mathcal{M}|^2}{(2\pi)^{3n}}\delta^4(p_a+p_b-\Sigma p_i)\prod_i\frac{d^3p_i}{2E_i} =$$

$$= \frac{1}{2\lambda^{1/2}(\hat{s},0,0)}\frac{\sum|\mathcal{M}|^2}{(2\pi)^5}\delta^4(k_3+k_4+k_2+k_1)\frac{d^3k_1}{2k_1^0}\frac{d^3k_2}{2k_2^0}dk_1^2\; dPS(k_1;p_1,p_2) \qquad (2.2)$$

with

$$\lambda(a,b,c) = a^2+b^2+c^2-2ab-2ac-2bc$$

Integrating over the phase space of the two final leptons,

$$\int \delta^4(k_1 - p_1 - p_2)\frac{d^3p_1}{2p_1^0}\frac{d^3p_2}{2p_2^0}\; 4(p_2^\mu p_1^\lambda + p_1^\mu p_2^\lambda - g^{\mu\lambda}\; p_1\cdot p_2) = \frac{2\pi}{3}(k_1^\mu k_1^\lambda - k_1^2 g^{\mu\lambda}) \quad (2.3)$$

and using the fact that $k_1^\mu A_\mu = 0$ from gauge invariance, the differential cross section can be written as follows:

$$\frac{d\hat{\sigma}}{d\hat{t}dk_1^2} = \frac{\alpha^2\alpha_s^2\alpha_z}{\hat{s}^2}\frac{16\pi^2}{3}\left(\frac{1}{k_1^2}\right)\left(\frac{1}{4}\cdot\frac{2}{64}\right)\sum_{\lambda_2,\lambda_3,\lambda_4}\left[\left(\sum_q Q_q g_v^q A_\mu\right)\left(\sum_q Q_q g_v^q A_\nu^*\right)(-g^{\mu\nu})\right] \quad (2.4)$$

where $\left(\frac{1}{4}\cdot\frac{2}{64}\right)$ comes out from spin average and colour factors, $\alpha_z \equiv \frac{\alpha}{sin^2\theta_w cos^2\theta_w}$, and

$$\hat{s} = (k_3 + k_4)^2$$

$$\hat{t} = (k_3 + k_1)^2$$

The calculation of the matrix elements A_μ follows from ref.13 where the general form of the vacuum polarization tensor allowed by Lorentz invariance, crossing symmetry and gauge invariance is obtained in the framework of double-dispersion representation for the amplitudes, instead of the usual Feynman parametrization. Using the same metric and notation as in ref.13, the $ggZ^0\gamma^*$ polarization tensor corresponding to the diagrams in fig.1a, can be written as

$$G_{\mu\nu\rho\sigma}(1234) = T_{\mu\nu\rho\sigma}(1234) + T_{\nu\mu\rho\sigma}(2134) + T_{\rho\nu\mu\sigma}(3214)$$

where for simplicity we have replaced k_i by i in the arguments and

$$\begin{aligned} T_{\mu\nu\rho\sigma}(1234) \;=\; & \int\frac{d^4P}{i\pi^2}\,Tr\Big\{\gamma_\mu\frac{\not P + i}{P^2+1}\gamma_\nu\frac{\not P - \not K_2 + i}{(P-K_2)^2+1}\gamma_\sigma \\ & \frac{\not P + \not K_1 + \not K_3 + i}{(P+K_1+K_3)^2+1}\gamma_\rho\frac{\not P + \not K_1 + i}{(P+K_1)^2+1}\Big\} \end{aligned} \quad (2.5)$$

Notice that as in ref.13, all momenta have been divided by m_q, i.e. $P = p/m_q$, $K_i = k_i/m_q$.

We define the following dimensionless scalar variables:

$$r = -\frac{1}{4}(K_1 + K_2)^2$$

$$s = -\frac{1}{4}(K_1 + K_3)^2$$

$$t = -\frac{1}{4}(K_1 + K_4)^2$$

and $(K_i)^2 = 4\mu_i$ $(i = 1,2,3,4)$. They are related by

$$r + s + t + \mu_1 + \mu_2 + \mu_3 + \mu_4 = 0$$

We choose K_3 and K_4 to be the (dimensionless) momenta of the initial gluons and we assume the following kinematics:

$$\begin{aligned} K_3 &= (0,0,-k,-ik) \\ K_4 &= (0,0,k,-ik) \\ K_2 &= (-q sin\theta, 0, -q cos\theta, ip) \\ K_1 &= (q sin\theta, 0, q cos\theta, i(2k-p)) \end{aligned} \quad (2.6)$$

The helicity vectors for circular polarization are :

$$a_3^{(\lambda_3)} = \frac{1}{\sqrt{2}}(-i\lambda_3, 1, 0, 0)$$

$$a_4^{(\lambda_4)} = \frac{1}{\sqrt{2}}(i\lambda_4, 1, 0, 0)$$

$$b_2^{(\lambda_2)} = \frac{1}{\sqrt{2}}(i\lambda_2 cos\theta, 1, -i\lambda_2 sin\theta, 0)$$

for the gluons and the Z^0, and

$$b_2^{(0)} = \frac{1}{m}(-p sin\theta, 0, -p cos\theta, -iq)$$

for the longitudinal polarization of the Z^0.

$a_3^{(\lambda_3)}$ and $a_4^{(\lambda_4)}$ specify right and left-handed circular polarizations states when $\lambda_3 = \lambda_4 = 1$ and $\lambda_3 = \lambda_4 = -1$ respectively for two incoming gluons.

We follow section 4 in ref.13 where the fully integrated expression of the polarization tensor is obtained in terms of logarithm and dilogarithm functions when two of the four photons are on the mass shell (the case $\mu_3 = \mu_4 = 0$). Then, for two incoming gluons, the following tensor is defined

$$G_{\mu\nu\rho\sigma}(1234)\left(a_3^{(\lambda_3)}\right)_\rho \left(a_4^{(\lambda_4)}\right)_\sigma = G_{\mu\nu}^{(-\lambda_3,-\lambda_4)}(1234)$$

and is obtained by

$$G_{\mu\nu}^{(\lambda_3,\lambda_4)}(1234) = \sum_{4perm}\sum_{i=1}^{4} g_i\left\{\frac{1}{2}(1+\lambda_3\lambda_4)D_+^{(i)}(1234) + \frac{1}{2}(1-\lambda_3\lambda_4)D_-^{(i)}(1234)\right\} L_{\mu\nu}^{(i)}(1234)$$

where $g_i = 1$ for $i = 1,2,3$ and $g_4 = \lambda_3$. The sum over permutations refers to the interchanges $(K_1,\mu) \leftrightarrow (K_2,\nu)$ and/or $(K_3,\lambda_3) \leftrightarrow (K_4,\lambda_4)$ and the amplitudes $D_\pm^{(i)}$ are listed in Appendix III of ref.13. The tensors $L_{\mu\nu}^{(i)}$ defined in ref.13 have the following expressions:

$$\begin{aligned} L_{\mu\nu}^{(1)}(1234) &= \frac{1}{4}\left[\frac{K_{2_\mu}K_{1_\nu}}{(K_1\cdot K_2)} - \delta_{\mu\nu}\right] \\ L_{\mu\nu}^{(2)}(1234) &= \frac{1}{2}N_\mu(1234)N_\nu(2134) \\ L_{\mu\nu}^{(3)}(1234) &= \frac{1}{2}N_\mu(1234)N_\nu(2143) \\ L_{\mu\nu}^{(4)}(1234) &= N_\mu(1234)\chi_\nu(1234) \end{aligned} \quad (2.7)$$

where

$$N_\mu(1234) = K_{3_\mu} - \frac{(K_1 \cdot K_3)}{(K_1 \cdot K_2)} K_{2_\mu}$$

$$\chi_\nu(1234) = \epsilon_{\nu\beta\gamma\delta} K_1^\beta K_2^\gamma K_3^\delta \qquad (2.8)$$

Using the symmetry properties of the $D_\pm^{(i)}$ amplitudes

$$D_\pm^{(1)}(1234) = D_\pm^{(1)}(2134) = D_\pm^{(1)}(1243) = D_\pm^{(1)}(2143)$$

$$D_\pm^{(2)}(1234) = D_\pm^{(2)}(2134)$$

$$D_\pm^{(3)}(1234) = D_\pm^{(3)}(2143)$$

$$D_\pm^{(4)}(1234) \textit{ has no symmetry properties}$$

we obtain $G_{\mu\nu}^{(-\lambda_3,-\lambda_4)}$ after summing over permutations. Multiplying then by the polarization vector $\left(b_2^{(\lambda_2)}\right)^*_\nu$ of the Z^0 ($\lambda_2 = 0, +1, -1$) we obtain our $G_\mu^{(\lambda_2,\lambda_3,\lambda_4)}$.

For $\lambda_2 = \pm 1$ the final expression can be written as:

$$G_\mu^{(\lambda_2,\lambda_3,\lambda_4)} = \frac{i}{4\sqrt{2urv}} \Big\{ E^{(1)}_{\lambda_2\lambda_3\lambda_4}(1234) N_\mu(1234) - E^{(1)}_{\lambda_2\lambda_4\lambda_3}(1243) N_\mu(1243)$$

$$+ E^{(2)}_{\lambda_2\lambda_3\lambda_4}(1234)\chi_\mu(1234) \Big\}$$

with

$$u = st - \mu_1\mu_2$$

$$v = (s+t)^2 - 4\mu_1\mu_2$$

and

$$\begin{aligned} E^{(1)}_{\lambda_2\lambda_3\lambda_4} &= \frac{1}{4}(\lambda_2 + \lambda_3 + \lambda_4 + \lambda_2\lambda_3\lambda_4) E^{(1)}_{+++} + \frac{1}{4}(-\lambda_2 + \lambda_3 + \lambda_4 - \lambda_2\lambda_3\lambda_4) E^{(1)}_{-++} \\ &+ \frac{1}{4}(\lambda_2 - \lambda_3 + \lambda_4 - \lambda_2\lambda_3\lambda_4) E^{(1)}_{+-+} + \frac{1}{4}(\lambda_2 + \lambda_3 - \lambda_4 - \lambda_2\lambda_3\lambda_4) E^{(1)}_{++-} \end{aligned}$$

$$\begin{aligned} E^{(2)}_{\lambda_2\lambda_3\lambda_4} &= \frac{1}{4}(1 + \lambda_2\lambda_3 + \lambda_2\lambda_4 + \lambda_3\lambda_4) E^{(2)}_{+++} + \frac{1}{4}(1 - \lambda_2\lambda_3 - \lambda_2\lambda_4 + \lambda_3\lambda_4) E^{(2)}_{-++} \\ &+ \frac{1}{4}(1 - \lambda_2\lambda_3 + \lambda_2\lambda_4 - \lambda_3\lambda_4) E^{(2)}_{+-+} + \frac{1}{4}(1 + \lambda_2\lambda_3 - \lambda_2\lambda_4 - \lambda_3\lambda_4) E^{(2)}_{++-} \end{aligned}$$

Then we have $E^{(1)}_{\lambda_2\lambda_3\lambda_4} = -E^{(1)}_{-\lambda_2-\lambda_3-\lambda_4}$ and $E^{(2)}_{\lambda_2\lambda_3\lambda_4} = E^{(2)}_{-\lambda_2-\lambda_3-\lambda_4}$

These 8 independent functions $E^{(1),(2)}_{\lambda_2\lambda_3\lambda_4}$ are related to the $D_\pm^{(i)}$ amplitudes as follows

$$E^{(1)}_{+++} = -AD_+^{(1)}(1234) + 8ru\left[-D_+^{(2)}(1234) + D_+^{(3)}(1234) + 2\sqrt{v}D_+^{(4)}(1234)\right]$$

$$E^{(1)}_{-++} = AD_+^{(1)}(1234) + 8ru\left[D_+^{(2)}(1234) - D_+^{(3)}(1234) + 2\sqrt{v}D_+^{(4)}(1234)\right]$$

$$E^{(1)}_{+-+} = -AD^{(1)}_{-}(1234) + 8ru\left[-D^{(2)}_{-}(1234) + D^{(3)}_{-}(1234) - 2\sqrt{v}D^{(4)}_{-}(1234)\right]$$

$$E^{(1)}_{++-} = -AD^{(1)}_{-}(1234) + 8ru\left[-D^{(2)}_{-}(1234) + D^{(3)}_{-}(1234) + 2\sqrt{v}D^{(4)}_{-}(1234)\right]$$

$$E^{(2)}_{+++} = -\sqrt{v}D^{(1)}_{+}(1234) - 8ru\left[D^{(4)}_{+}(2134) + D^{(4)}_{+}(2143)\right]$$

$$E^{(2)}_{-++} = -\sqrt{v}D^{(1)}_{+}(1234) + 8ru\left[D^{(4)}_{+}(2134) + D^{(4)}_{+}(2143)\right]$$

$$E^{(2)}_{+-+} = -\sqrt{v}D^{(1)}_{-}(1234) + 8ru\left[D^{(4)}_{-}(2134) - D^{(4)}_{-}(2143)\right]$$

$$E^{(2)}_{++-} = -\sqrt{v}D^{(1)}_{-}(1234) - 8ru\left[D^{(4)}_{-}(2134) - D^{(4)}_{-}(2143)\right]$$

with $A = -4u - 2(s+\mu_2)(s-t)$

Similarly for $\lambda_2 = 0$,

$$G_{\mu}^{(0,\lambda_3,\lambda_4)} = \frac{i}{4\sqrt{2urv}}\{E^{(1)}_{0\lambda_3\lambda_4}(1234)N_{\mu}(1234) + E^{(1)}_{0\lambda_4\lambda_3}(1243)N_{\mu}(1243) + E^{(2)}_{0\lambda_3\lambda_4}(1234)\chi_{\mu}(1234)\}$$

$$E^{(1)}_{0\lambda_3\lambda_4}(1234) = E^{(1)}_{0-\lambda_3-\lambda_4} = \frac{1}{2}(1+\lambda_3\lambda_4)E^{(1)}_{0++} + \frac{1}{2}(1-\lambda_3\lambda_4)E^{(1)}_{0+-}$$

$$E^{(2)}_{0\lambda_3\lambda_4}(1234) = -E^{(2)}_{0-\lambda_3-\lambda_4} = \frac{1}{2}(\lambda_3+\lambda_4)E^{(2)}_{0++} + \frac{1}{2}(\lambda_3-\lambda_4)E^{(2)}_{0+-}$$

where

$$E^{(1)}_{0++} = \frac{8i\sqrt{ur(-\mu_2)}}{\sqrt{2}}\left\{D^{(1)}_{+}(1234) - \frac{1}{(s+t)}\left[(v+B)D^{(2)}_{+}(1234) + (v-B)D^{(3)}_{+}(1234)\right]\right\}$$

$$E^{(1)}_{0+-} = \frac{8i\sqrt{ur(-\mu_2)}}{\sqrt{2}}\left\{D^{(1)}_{-}(1234) - \frac{1}{(s+t)}\left[(v+B)D^{(2)}_{-}(1234) + (v-B)D^{(3)}_{-}(1234)\right]\right\}$$

$$E^{(2)}_{0++} = \frac{-8i\sqrt{ur(-\mu_2)}}{\sqrt{2}(s+t)}\left[(v+B)D^{(4)}_{+}(2134) - (v-B)D^{(4)}_{+}(2143)\right]$$

$$E^{(2)}_{0+-} = \frac{-8i\sqrt{ur(-\mu_2)}}{\sqrt{2}(s+t)}\left[(v+B)D^{(4)}_{-}(2134) + (v-B)D^{(4)}_{-}(2143)\right]$$

with $B = (s-t)(s+t+2\mu_1)$

The evaluation of the amplitude A_μ is numerically complicated, for large quark masses. This contribution however decreases with m_q [15] and can be neglected for the case of the top quark as it is shown in fig.2 where the contribution of a given quark to the differential cross section is plotted for different masses. For light quarks one can use the small quark mass limits of the trascendental functions appearing in the amplitudes $D_\pm^{(i)}$ which are explicitly given in Appendix A. Taking into account that $A_\mu \equiv 2\frac{i\pi^2}{(2\pi)^4}G_\mu$ (the factor 2 is needed to include the effect of the other 3 diagrams obtained by permutation of gluon lines in the diagrams of fig.(1a)), and neglecting the contribution of the top quark ($m_{top} > 120$ Gev), we obtain from eq. 2.4 the differential cross-section for the process $gg \to Z^0\gamma^* \to Z^0\mu^+\mu^-$.

3 Cross Section for $pp \to Z^0\gamma^* + X \to Z^0\mu^+\mu^- + X$

The diagrams contributing to the $q-\bar{q}$ subprocess are shown in fig.1b, and the matrix element is given by

$$|\mathcal{M}| = Q_q \frac{e^2\, g}{cos\theta_w} \frac{1}{k_1^2} \bar{u}(p_1)\gamma^\alpha v(p_2)\ \bar{v}(q_b)(g_q^v - g_q^a\gamma_5)\left\{\frac{\gamma_\alpha \not{q} \not{\epsilon}_z^*}{q^2} + \frac{\not{\epsilon}_z^* \not{p}\gamma_\alpha}{p^2}\right\} u(q_a) \tag{3.1}$$

Following the same steps as in section 2, after integration over the two muon phase space, the differential cross-section can be written as follows:

$$\frac{d\hat{\sigma}}{d\hat{t}dk_1^2} = \frac{\alpha^2\alpha_z}{\hat{s}^2}\frac{8}{3}\left(\frac{1}{k_1^2}\right)\left(\frac{1}{4}\cdot\frac{1}{3}\right) Q_q^2(g_v^2+g_a^2)\left\{-M_Z^2k_1^2\left(\frac{1}{\hat{t}^2}+\frac{1}{\hat{u}^2}\right)+\frac{\hat{u}}{\hat{t}}+\frac{\hat{t}}{\hat{u}}+\frac{2\hat{s}(M_Z^2+k_1^2)}{\hat{u}\hat{t}}\right\} \tag{3.2}$$

where $\left(\frac{1}{4}\cdot\frac{1}{3}\right)$ is the initial spin and colour average factor.

A further integration over the parton structure functions will give us the contributions to the proton-proton cross section, namely

$$\frac{d\sigma}{dM_{Z\gamma^*}^2 dk_1^2} = \frac{1}{s}\int_{-y_{cut}}^{y_{cut}} dy \left[\sum_{ij} f^i(x_1,Q^2) f^j(x_2,Q^2)\right]\frac{d\hat{\sigma}}{dk_1^2}$$

where

$$x_1 = \sqrt{\frac{\hat{s}}{s}}\, e^y, \qquad x_2 = \sqrt{\frac{\hat{s}}{s}}\, e^{-y} \quad and \quad Q^2 = \frac{\hat{s}}{4}$$

with

$$\frac{d\hat{\sigma}}{dk_1^2} = \int_{-z_1}^{z_0} \frac{d\hat{\sigma}}{dz^* dk_1^2} = \int_{-z_1}^{z_0} \frac{\lambda^{1/2}(\hat{s}, m_Z^2, k_1^2)}{2}\frac{d\hat{\sigma}}{d\hat{t}dk_1^2}$$

and $z^* = cos\theta^*$, θ^* being the parton-parton center of mass scattering angle. The two limits z_0 and z_1 depend on the rapidity cut and they have the following expressions:

$$z_0 = min[1, \beta_K^{-1} tgh(y_{cut} - y), \beta_Z^{-1} tgh(y_{cut} + y)],$$
$$z_1 = min[1, \beta_K^{-1} tgh(y_{cut} + y), \beta_Z^{-1} tgh(y_{cut} - y)]$$

where

$$\beta_K = \frac{\lambda^{1/2}(\hat{s}, m_Z^2, k_1^2)}{\hat{s} - M_Z^2 + k_1^2} \qquad and \qquad \beta_Z = \frac{\lambda^{1/2}(\hat{s}, m_Z^2, k_1^2)}{\hat{s} + M_Z^2 - k_1^2}$$

We have computed the invariant mass distribution of the two final leptons for different values of $M_{Z\gamma^*}$ at LHC and SSC energies using the Duke and Owens parton distribution functions with $\Lambda = 0.2$ Gev [16]. We show in figs. 3a and 3b the *gluon – gluon* contribution compared with the $q\bar{q}$ contribution for a rapitity cut of 2.5 . As we have already mentioned the gluonic contribution is much smaller, both at the SSC and at the LHC energy . This is due to the fact that there is no contribution of the axial coupling to the box diagram for this particular process and that the axial coupling is larger than the vector coupling.

4 Comparison with the signal

It is well known that the main contribution to the production of the intermediate mass Higgs in hadron collisions is via gluon fusion. The cross section for production of a Higgs boson decaying into $Z^0\mu^+\mu^-$ via a virtual Z^* can then be written as follows [17, 18]

$$\frac{d\sigma(pp \to gg + X \to H + X \to Z^0\mu^+\mu^- + X)}{dQ_1^2 dy} = \frac{G_F \pi}{32\sqrt{2}} \left(\frac{\alpha_s}{\pi}\right)^2 |\eta_{gg}|^2 \tau g(x_1, Q^2) g(x_2, Q^2)$$
$$\frac{1}{\Gamma_H} \frac{M_H G_F}{8\pi\sqrt{2}} \frac{1}{(Q_1^2 - M_Z^2)^2 + M_Z^2 \Gamma_Z^2} \left(\frac{M_Z \Gamma_Z}{\pi}\right) (B_{Z\to\mu^+\mu^-})$$
$$\cdot \lambda^{1/2}\left(M_H^2, Q_1^2, M_Z^2\right) \left[1 + \frac{Q_1^4}{M_H^4} + \frac{M_Z^4}{M_H^4} - 2\frac{Q_1^2}{M_H^2} - 2\frac{M_Z^2}{M_H^2} + 10\frac{Q_1^2 M_Z^2}{M_H^4}\right]$$

where the narrow width approximation for the Higgs boson has been used. The complex function η_{gg} is the amplitude for the process *gluon – gluon* $\longrightarrow H$, defined so that the decay width of the Higgs boson into two gluons is given by

$$\Gamma(H \to gluon\ gluon) = \frac{G_F M_H^3}{4\pi\sqrt{2}} \left[\frac{\alpha_s}{\pi}\right]^2 |\eta_{gg}|^2$$

The $\mu^+\mu^-$ invariant mass distribution for the signal is shown in figs.4a-d for $\sqrt{s} =$ 16 and 40 Tev and for two different values of the Higgs mass, 130 and 150 Gev. In order to compare the signal with the backgrounds from figs.3a and 3b, we integrate the $q\bar{q}$ contribution over a $M_{Z\gamma^*}$ bin of 5 and 10 Gev and the result is shown in figs.4a-d together with the signal.

A cut of 15-20 Gev in the invariant mass of the $\mu^+\mu^-$ pair, will reduce considerably the background. Notice that also the signal will be reduced, however . Indeed this reduction will place limits on the range of Higgs masses for which the 4 lepton channel can give an acceptable signal to background ratio. We show in fig.5 the probability that, in the decay of a Higgs boson into Z^0Z^* , the two leptons from the off-mass-shell Z have an invariant mass larger than 10, 20 or 50 GeV. This plot shows that with a cut of 20 GeV on the non-resonant lepton pair, the signal for a Higgs boson of 130 GeV is reduced by 50% relative to the one for Z^*Z^* . Since the total number of events in two lepton pairs at LHC for a Higgs boson of mass 130 GeV is $\approx$ 100-150 events, this confirms previous estimates [10] that this channel cannot be used for Higgs boson masses less than 130 GeV.

5 Conclusions

We have calculated the contribution of gluon-gluon scattering to the production of a $Z^0\gamma^*$ pair in proton proton collisions at center of mass energies of 16 and 40 TeV. This contribution is smaller than the one from quark-antiquark annihilation by more than one order of magnitude and therefore it cannot constitute a relevant background for the detection of an intermediate mass Higgs boson decaying into two lepton pairs.

Acknowledgements

We thank B.De Tollis for many enlightening discussions and for a critical reading of the manuscript.

Appendix A

We define the trascendental functions used in the calculation

$$
\begin{aligned}
B(r) &= \frac{1}{2}\int_0^1 dy\; ln\{1 - i\epsilon - 4ry(1-y)\} \\
&= \left(1-\frac{1}{r}\right)^{1/2} sinh^{-1}\sqrt{-r} - 1 && (r<0) \\
&= \left(\frac{1}{r}-1\right)^{1/2} sin^{-1}\sqrt{r} - 1 && (0<r<1) \qquad \text{(A.1)} \\
&= \left(1-\frac{1}{r}\right)^{1/2} cosh^{-1}\sqrt{r} - 1 - \frac{\pi i}{2}\left(1-\frac{1}{r}\right)^{1/2} && (1<r)
\end{aligned}
$$

$$
\begin{aligned}
T(r) &= \int_0^1 \frac{dy}{4y(1-y)}\; ln\{1 - i\epsilon - 4ry(1-y)\} \\
&= \left(sinh^{-1}\sqrt{-r}\right)^2 && (r<0) \\
&= -\left(sin^{-1}\sqrt{r}\right)^2 && (0<r<1) \qquad \text{(A.2)} \\
&= \left(cosh^{-1}\sqrt{r}\right)^2 - \frac{1}{4}\pi^2 - i\pi cosh^{-1}\sqrt{r} && (1<r)
\end{aligned}
$$

$$
T_1(r,\mu_1,\mu_2) = \frac{r_{12}}{2\sqrt{v}}\left\{I_2^G(1,-4\mu_1,y_1) + I_2^G(1,-4\mu_2,y_2) - I_2^G(1,4r,y_3)\right\} \qquad \text{(A.3)}
$$

where

$$
r_{12} = r + \mu_1 + \mu_2
$$

$$
y_1 = \frac{r_{12} - 2\mu_2 + \sqrt{v}}{2\sqrt{v}}; \quad y_2 = \frac{r_{12} - 2\mu_1 + \sqrt{v}}{2\sqrt{v}}; \quad y_3 = \frac{r_{12} + \sqrt{v}}{2\sqrt{v}}. \qquad \text{(A.4)}
$$

and I_2^G is the function defined by Glover et al. in ref.14:

$$
\begin{aligned}
I_2^G(a,b,y_0) &= \int_0^1 \frac{dy}{y-y_0}\Big(ln[a - i\epsilon - by(1-y)] - ln[a - i\epsilon - by_0(1-y_0)]\Big) \qquad \text{(A.5)} \\
&= Sp\left(\frac{y_0}{y_0 - z_1}\right) - Sp\left(\frac{y_0 - 1}{y_0 - z_1}\right) + Sp\left(\frac{y_0}{y_0 - z_2}\right) - Sp\left(\frac{y_0 - 1}{y_0 - z_2}\right)
\end{aligned}
$$

with

$$z_1 = \frac{1}{2}\left(1+\sqrt{1-\frac{4(a-i\epsilon)}{b}}\right), \quad z_2 = 1 - z_1$$

$$I_1(r,s,\mu_1,\mu_2) = \frac{1}{4a_1}\Bigg\{ I_1^G(4r,0,y_{1+}+\beta_1) - I_1^G(4r,0,y_{1-}+\beta_1) - I_1^G\left(-4t_2,-4s_1,\frac{y_{1+}}{1-\beta_1}\right)$$
$$+I_1^G\left(-4t_2,-4s_1,\frac{y_{1-}}{1-\beta_1}\right) + I_1^G\left(4s_1,-4s_1,-\frac{y_{1+}}{\beta_1}\right) - I_1^G\left(4s_1,-4s_1,-\frac{y_{1-}}{\beta_1}\right)$$
$$-I_1^G(4r,0,y_{2+}+\beta_2) + I_1^G(4r,0,y_{2-}+\beta_2) + I_1^G\left(-4t_2,-4s_1,\frac{y_{2+}}{1-\beta_2}\right)$$
$$-I_1^G\left(-4t_2,-4s_1,\frac{y_{2-}}{1-\beta_2}\right) - I_1^G\left(4s_1,-4s_1,-\frac{y_{2+}}{\beta_2}\right) + I_1^G\left(4s_1,-4s_1,-\frac{y_{2-}}{\beta_2}\right)$$
$$+I_2^G\left(1,-4\mu_2,\frac{y_{1+}}{1-\beta_1}\right) - I_2^G\left(1,-4\mu_2,\frac{y_{1-}}{1-\beta_1}\right) - I_2^G\left(1,4s,-\frac{y_{1+}}{\beta_1}\right) +$$
$$I_2^G\left(1,4s,-\frac{y_{1-}}{\beta_1}\right) + I_2^G(1,4r,y_{2+}+\beta_2) - I_2^G(1,4r,y_{2-}+\beta_2) - I_2^G\left(1,-4\mu_2,\frac{y_{2+}}{1-\beta_2}\right)$$
$$+ I_2^G\left(1,-4\mu_2,\frac{y_{2-}}{1-\beta_2}\right) + I_2^G\left(1,-4\mu_1,-\frac{y_{2+}}{\beta_2}\right) - I_2^G\left(1,-4\mu_1,-\frac{y_{2-}}{\beta_2}\right)\Bigg\} \quad \text{(A.6)}$$

where

$$a_1 = \sqrt{1+\frac{u}{rs^2}}; \quad \beta_1 = \frac{s}{s_2}; \quad y_{1\pm} = -\frac{s}{2s_2}(1\pm a_1)$$
$$\beta_2 = \frac{r_{12}-2\mu_1-\sqrt{v}}{2r}; \quad y_{2\pm} = \frac{\mu_1 r + (\mu_1-\mu_2)s_1 + s_1\sqrt{v} \mp rsa_1}{r(r_{12}+2s+\sqrt{v})}$$

and [14]

$$\begin{aligned} I_1^G(a,b,y_0) &= \int_0^1 \frac{dy}{y-y_0}[ln(ay+b-i\epsilon) - ln(ay_0+b-i\epsilon)] \\ &= Sp\left(\frac{y_0}{y_0-z}\right) - Sp\left(\frac{y_0-1}{y_0-z}\right) \end{aligned} \quad \text{(A.7)}$$

with

$$z = -\frac{b-i\epsilon}{a}$$

$$I_2(s,t,\mu_1,\mu_2) = \frac{1}{2a_2}\Bigg\{ I_2^G(1,-4\mu_1,x_+) + I_2^G(1,-4\mu_2,x_+) - I_2^G(1,4s,x_+)$$
$$-I_2^G(1,4t,x_+) + ln\left(-\frac{x_-}{x_+}\right)\Big[ln(1-i\epsilon+4\mu_1 x_+x_-) + ln(1-i\epsilon+4\mu_2 x_+x_-)$$
$$- ln(1-i\epsilon-4sx_+x_-) - ln(1-i\epsilon-4tx_+x_-)\Big]\Bigg\} \quad \text{(A.8)}$$

with

$$a_2 = \sqrt{1+\frac{r}{u}}; \quad x_\pm = \frac{1\pm a_2}{2}.$$

In the limit that the quark mass is smaller than all the other quantities they have the following simpler expression

$$B(r) = \frac{1}{2}ln(|4r|) - 1 - \frac{1}{2}i\pi\theta(r) \tag{A.9}$$

and the difference

$$B(r) - B(-\mu_2) = \frac{1}{2}ln\left(\frac{|r|}{-\mu_2}\right) - \frac{i\pi}{2}[\theta(r) - 1]$$

becomes independent of the quark mass.

$$T(r) = \frac{1}{4}ln^2(|4r|) - \theta(r)\left[\frac{\pi^2}{4} + \frac{i\pi}{2}ln(|4r|)\right] \tag{A.10}$$

$$T_1(r, \mu_1, \mu_2) \simeq \frac{r_{12}}{\sqrt{v}}\left\{Sp\left(-\frac{y_2 - 1}{y_1}\right) - Sp\left(-\frac{y_2}{y_1 - 1}\right) + \frac{1}{2}ln\left(\frac{y_1}{y_1 - 1}\right) ln\left(\frac{y_1(y_1 - 1)}{y_2(y_2 - 1)}\right)\right\} \tag{A.11}$$

$$\begin{aligned} I_1(r, s, \mu_1, \mu_2) \simeq \frac{1}{4}\Big\{ & 2Sp\left(\frac{s}{s_1}\right) + 2Sp\left(\frac{s}{s_2}\right) + \frac{1}{2}ln^2(4r) + ln(4r)ln\left(\frac{s^2}{\mu_1\mu_2}\right) \\ & + ln^2\left(\frac{s}{s_1}\right) + ln^2\left(\frac{s}{s_2}\right) - \frac{1}{2}ln^2\left(\frac{\mu_1}{\mu_2}\right) + \frac{\pi^2}{6} \\ & + i\pi\left[ln(4r) + ln\left(\frac{\mu_1 s}{s_1^2}\right) + ln\left(\frac{\mu_2 s}{s_2^2}\right)\right]\Big\} \end{aligned} \tag{A.12}$$

$$\begin{aligned} I_2(s, t, \mu_1, \mu_2) \simeq \frac{1}{2}\Big\{ & Sp\left(-\frac{u}{rs}\right) + Sp\left(-\frac{u}{rt}\right) - Sp\left(\frac{u}{\mu_1 r}\right) - Sp\left(\frac{u}{\mu_2 r}\right) \\ & + ln\left|\frac{1}{4s}\right| ln\left(1 + \frac{u}{rs}\right) + ln\left|\frac{1}{4t}\right| ln\left(1 + \frac{u}{rt}\right) \\ & - ln\left|\frac{1}{4\mu_1}\right| ln\left(1 - \frac{u}{\mu_1 r}\right) - ln\left|\frac{1}{4\mu_2}\right| ln\left(1 - \frac{u}{\mu_2 r}\right) \\ & - i\pi\left[2ln\left(\frac{r}{4u}\right) + ln\left(1 - \frac{u}{\mu_1 r}\right) + ln\left(1 - \frac{u}{\mu_2 r}\right)\right]\Big\} \end{aligned} \tag{A.13}$$

The functions $T(r)$, $I_1(r, s, \mu_1, \mu_2)$ and $I_2(s, t, \mu_1, \mu_2)$ are quark mass dependent but in this limits of small quark masses, they appear in the calculation in two combinations that are independent of m_q. These combinations E_1 and E_2 and their small m_q limit are defined below:

$$
\begin{aligned}
E_1(r, s, \mu_1, \mu_2) &\equiv I_1(r, s, \mu_1, \mu_2) - \frac{1}{2}\Big[T(r) - T(-\mu_1) - T(-\mu_2)\Big] - T(s) \\
&\simeq \frac{1}{4}\Bigg\{2Sp\left(\frac{s}{s_1}\right) + 2Sp\left(\frac{s}{s_2}\right) + \frac{1}{2}ln\left(\frac{s}{\mu_1}\right) ln\left(\frac{r^2}{\mu_1 s}\right) \\
&+\frac{1}{2}ln\left(\frac{s}{\mu_2}\right) ln\left(\frac{r^2}{\mu_2 s}\right) + ln^2\left(\frac{s}{s_1}\right) + ln^2\left(\frac{s}{s_2}\right) \\
&- \frac{1}{2}ln^2\left(\frac{\mu_1}{\mu_2}\right) - \frac{\pi^2}{3} + 2i\pi ln\left(-\frac{rs}{s_1 s_2}\right)\Bigg\}
\end{aligned}
\tag{A.14}
$$

$$
\begin{aligned}
E_2(s, t, \mu_1, \mu_2) &\equiv I_2(s, t, \mu_1, \mu_2) - T(s) - T(t) - T(-\mu_1) + T(-\mu_2) \\
&\simeq \frac{1}{2}\Bigg\{Sp\left(-\frac{u}{rs}\right) + Sp\left(-\frac{u}{rt}\right) - Sp\left(\frac{u}{\mu_1 r}\right) - Sp\left(\frac{u}{\mu_2 r}\right) \\
&+\frac{1}{2}ln^2\left(-\frac{rs}{s_1 s_2}\right) + \frac{1}{2}ln^2\left(-\frac{rt}{t_1 t_2}\right) - \frac{1}{2}ln^2\left(-\frac{\mu_1 r}{s_1 t_1}\right) \\
&-\frac{1}{2}ln^2\left(-\frac{\mu_2 r}{s_2 t_2}\right) + ln\left(\frac{s_1}{t_2}\right) ln\left(\frac{t_1}{s_2}\right) - \pi^2 \\
&+ i\pi\left[ln\left(\frac{u}{s_1 s_2}\right) + ln\left(\frac{u}{t_1 t_2}\right)\right]\Bigg\}
\end{aligned}
\tag{A.15}
$$

References

[1] C.Rubbia, *Perspectives for a Hadron Collider in the LEP Tunnel*, CERN Seminar, November 6th, 1989.

[2] J.F.Gunion, G.L.Kane and J.Wudka, Nucl. Phys. B299 (1988) 231.

[3] J.F.Gunion, H.E.Haber, G.L.Kane and S.Dawson. *The Higgs hunter's guide*, report UCD-89-4, SCIPP-89/13, BNL-41644, (June 1989).

[4] I.Montvay, *Non Perturbative Aspects of the Higgs Sector in the Standard Electroweak Theory* DESY 88-158, published in the Proceedings of the 7th INFN Eloisatroon Workshop, Erice, June 1988.

[5] J.Ellis and G.L.Fogli, Phys.Lett. B249 (1990) 543.

[6] H.Nilles, Phys. Rep. 110 (1984) 1;
H.Haber and G.Kane, Phys. Rep. 117 (1985) 75;
R. Barbieri, Riv. N. Cimento 11 (1988), 1.

[7] J.Ellis, G.Ridolfi and F.Zwirner, *Radiative corrections to the masses of supersymmetric Higgs bosons*, CERN-TH-5946-90, November 1990.

[8] R. Barbieri, M.Frigeni and F.Caravaglios, *The Supersymmetric Higgs for Heavy Superpartners*, IFUP-TH 46/90, December 1990
R. Barbieri and M.Frigeni, *The Supersymmetric Higgs Searches at LEP after Radiative Corrections*, IFUP-TH 2/91, January 1991.

[9] U. Amaldi, W. de Boer and H. Furstenau, *Compariosn of Grand Unified Theories with Electroweak ans Strong Coupling Constants measured at LEP*, CERN-PPE/91-44, 22 March 1991.

[10] D.Froidevaux,*Experimental Review of the Search for the Higgs Boson*, Proceedings of the EFCA/LHC Workshop, Aachen, 4-9 October 1990;
M.Della Negra et al., *Search for* $H \to Z^*Z^* \to 4$ *leptons at LHC*, Proceedings of the EFCA/LHC Workshop, Aachen, 4-9 October 1990.

[11] J.F.Gunion, P.Kalyniak, M.Soldate and P.Galison, Phys.Rev.D34 (1986) 101.

[12] A.Grau, G.Pancheri and Y.Srivastava, Physics Letters B247 (1990) 611.

[13] V.Costantini, B.De Tollis and G.Pistoni, Nuovo Cimento 2A (1971) 733.

[14] E.W.N.Glover and J.J.Van der Bij, Nucl. Phys. B231 (1989) 561.

[15] E.W.N.Glover and J.J.Van der Bij, Phys. Lett. B206 (1988) 701.

[16] D.W.Duke and J.F.Owens, Phys. Rev. D30 (1984) 49.

[17] A. Grau, G.Pancheri and R.J.N.Phillips, Phys.Lett. B251 (1990) 293.

[18] R.N.Cahn, Rep. Prog. Phys. 52 (1989) 389.

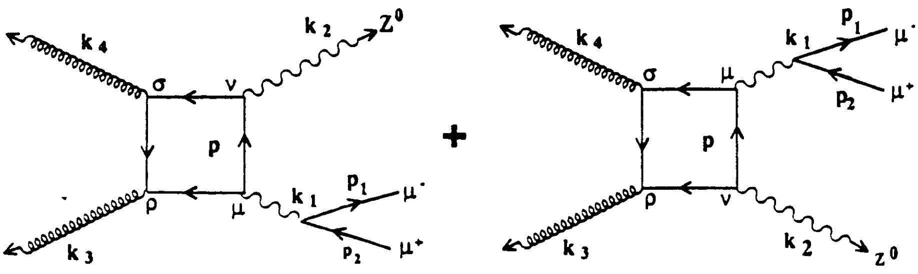

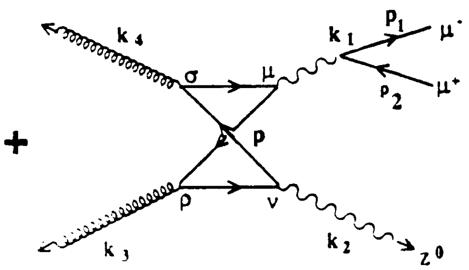

+ Permutation of gluon lines

Fig.1a Feynman diagrams for the process $gg \to Z^0\gamma^*$

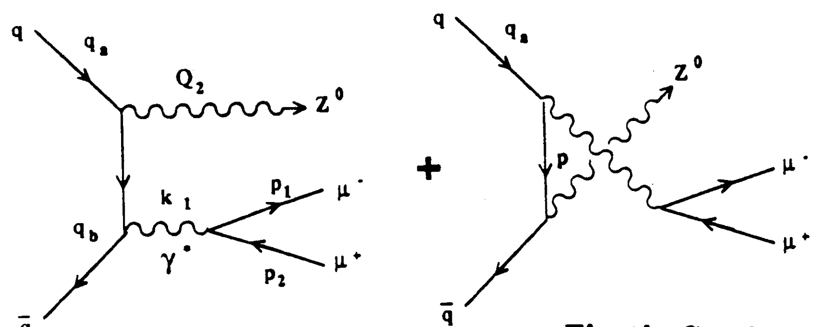

Fig.1b Graphs contributing to the process $q\bar{q} \to Z^0\gamma^*$

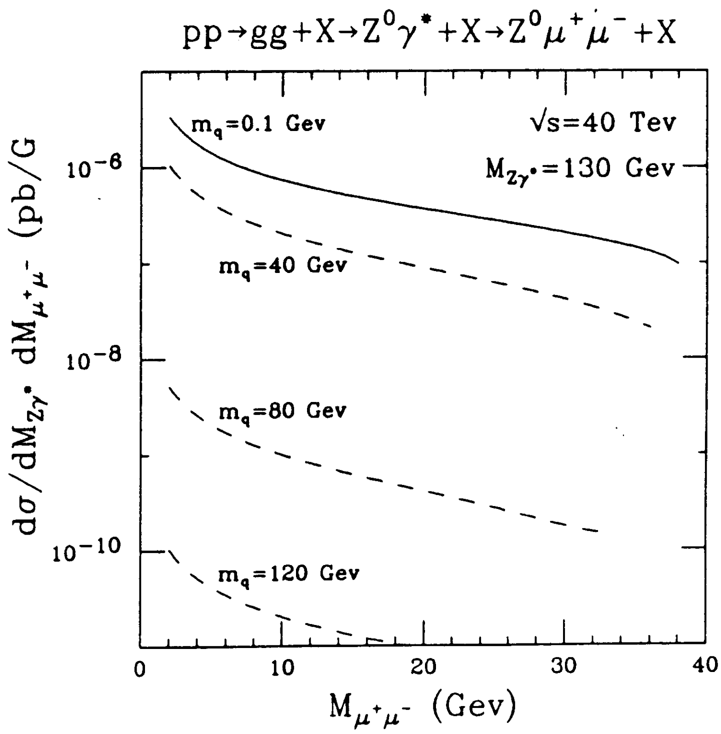

Fig.2 Contribution of a given quark to the differential cross-section for $pp \to gg \to Z^0\gamma^* \to Z^0\mu^+\mu^-$ for different quark masses.

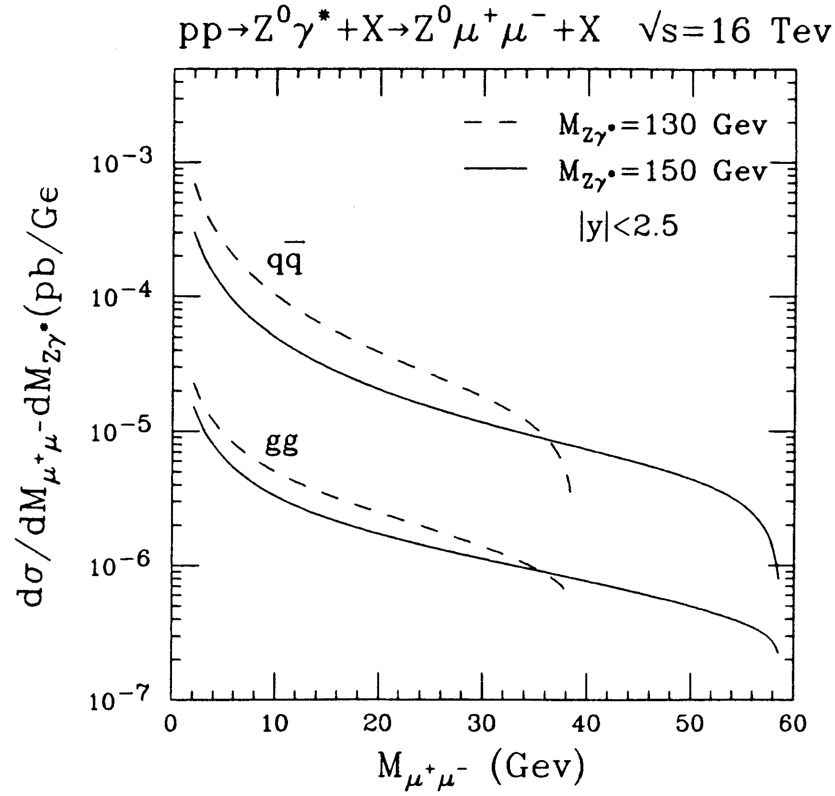

Fig.3a Differential cross-section for $pp \to Z^0\gamma^* \to Z^0\mu^+\mu^-$ at $\sqrt{s} = 16$ Tev.

$q\bar{q}$ and *gluon gluon* contributions are shown separately for two different values of $M_{Z\gamma^*}$: 130 Gev (dashed line) and 150 Gev (full line) and for a rapidity cut of 2.5.

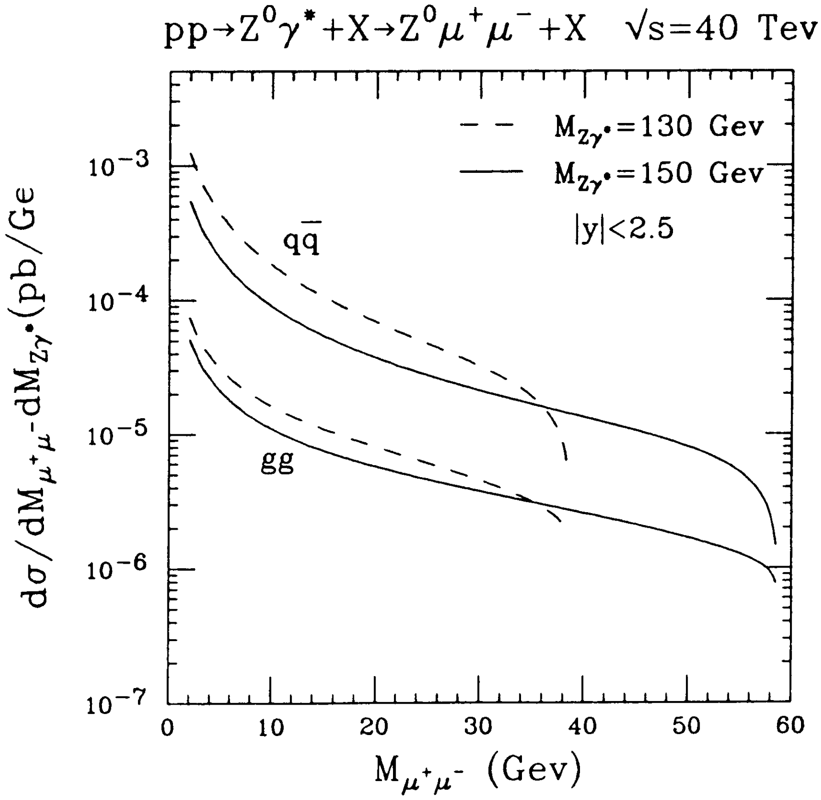

Fig.3b Same as Fig.3a for $\sqrt{s} = 40$ Tev.

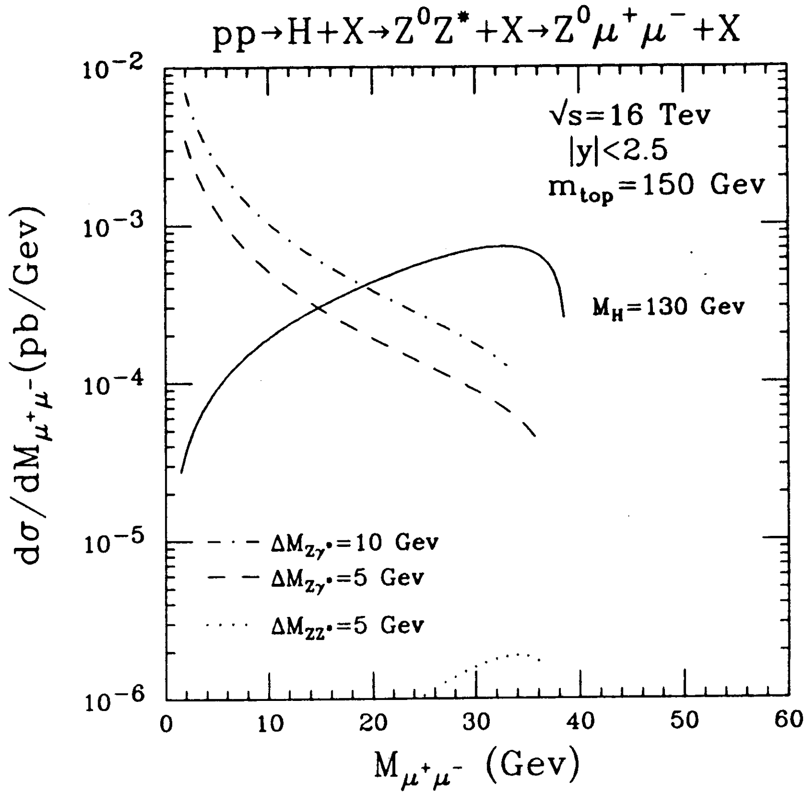

Fig.4a $\mu^+\mu^-$ invariant mass distribution for $pp \to H \to Z^0Z^* \to Z^0\mu^+\mu^-$ at $\sqrt{s} =$ 16 Tev and for $M_H = 130$ Gev (full line). Also shown are the contributions of $q\bar{q}$ background of fig.3 integrated over a $M_{Z\gamma^*}$ interval of 5 (dashed line) and 10 (dot-dashed line) Gev around $M_{Z\gamma^*} = M_H$. A value of $m_{top} = 150$ Gev has been used in the calculation of the signal. The dotted lines indicate the cross-section from the process $pp \to q\bar{q} + X \to Z^0Z^* \to Z^0\mu^+\mu^-$.

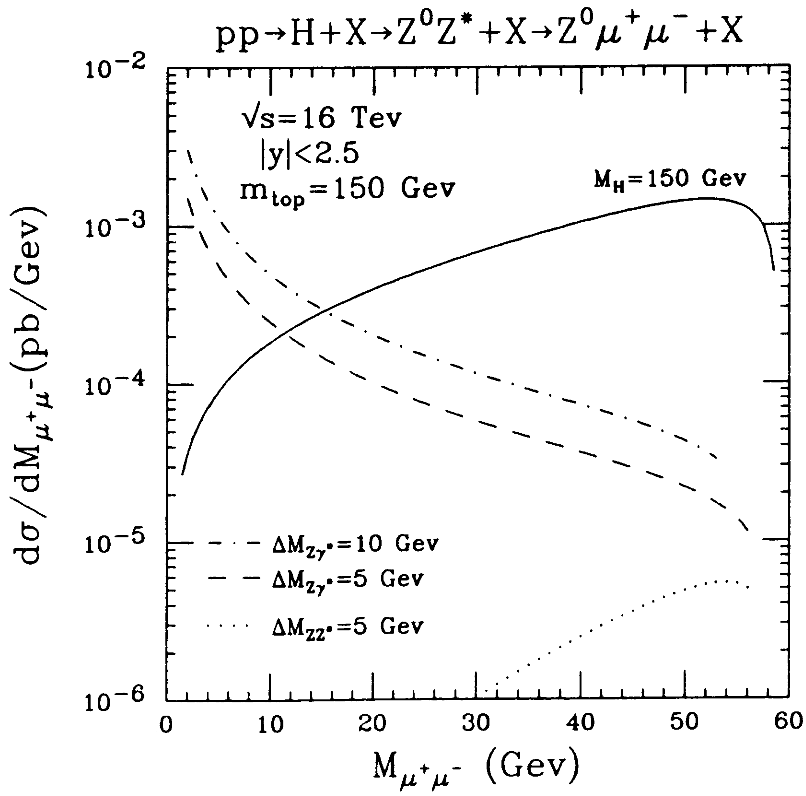

Fig.4b Same as fig.4a for $M_H = 150$ Gev.

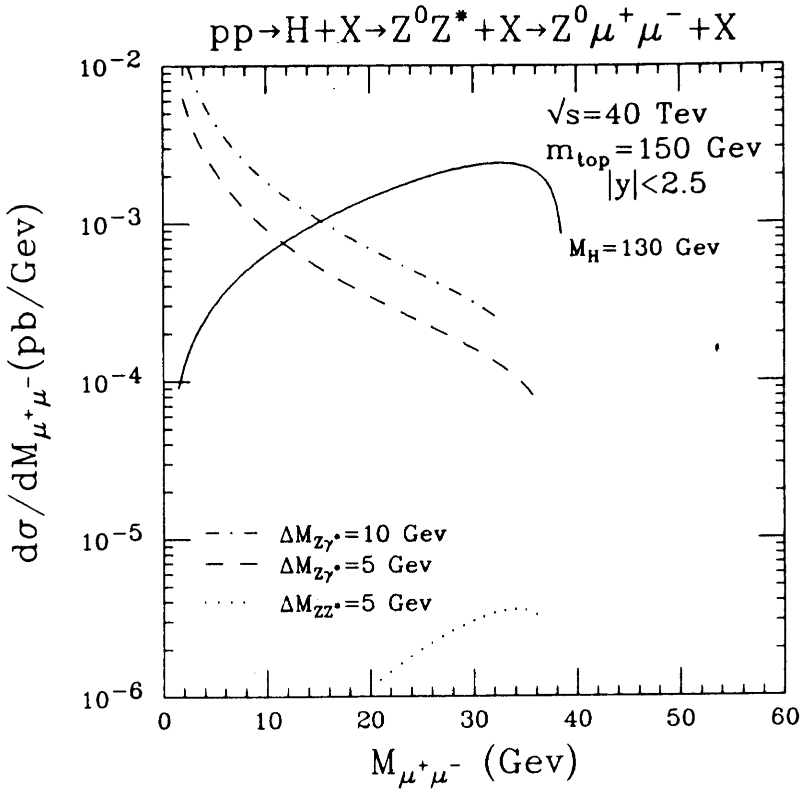

Fig.4c As in fig.4a with $\sqrt{s} = 40$ Tev.

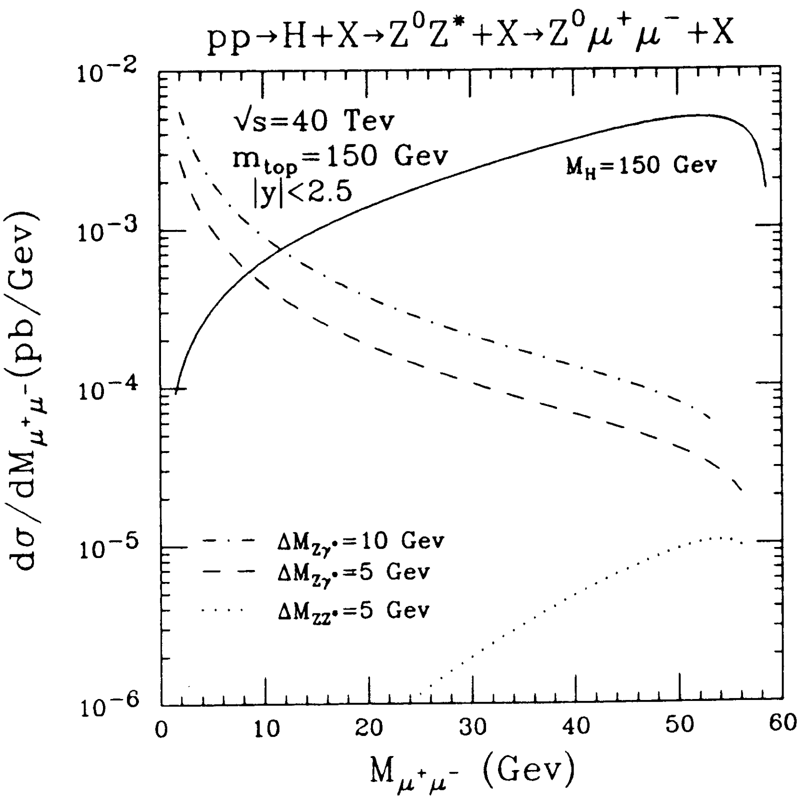

Fig.4d As in fig.4a for $M_H = 150$ Gev and $\sqrt{s} = 40$ Tev.

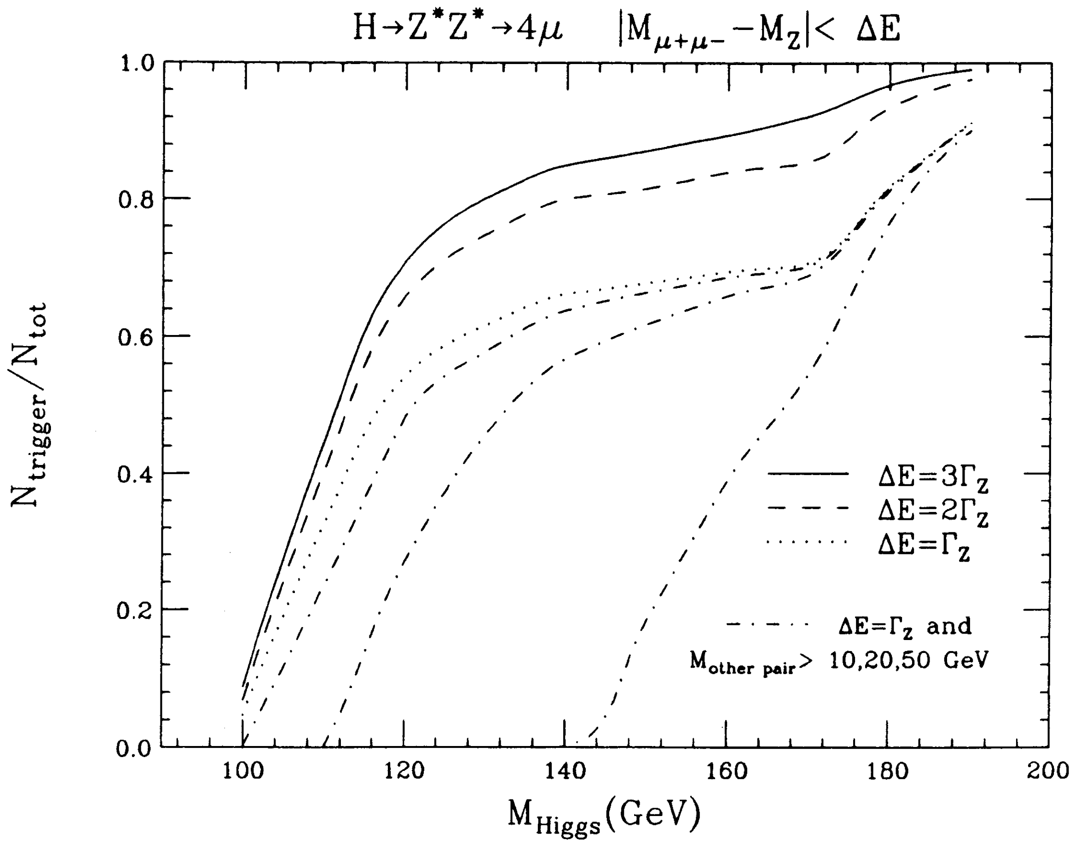

Fig.5 Probability that in the decay $H \rightarrow 4\mu$ the invariant mass of a μ-pair is larger than 10, 20 or 50 Gev (dot-dashed line), the other two muons being constrained to have an invariant mass close to M_Z, *i.e.* $M_Z - \Gamma_Z < M_{\mu^+\mu^-} < M_Z + \Gamma_Z$. Also shown are the probabilities that one of the 2 μ-pairs have an invariant mass

$$M_Z - 3\Gamma_Z < M_{\mu^+\mu^-} < M_Z + 3\Gamma_Z \ (full\ line)$$

$$M_Z - 2\Gamma_Z < M_{\mu^+\mu^-} < M_Z + 2\Gamma_Z \ (dashed\ line)$$

$$or\ M_Z - \Gamma_Z < M_{\mu^+\mu^-} < M_Z + \Gamma_Z \ (dotted\ line)$$

without any constraints on the other μ-pair.